Check for updates

Reactivity of Mg(AlMe₄)₂ towards neutral tris(pyrazolyl)alkanes†

Felix Kracht, Christoph Stuhl, Cäcilia Maichle-Mössmer and Reiner Anwander [ID] *

Various new tris(pyrazolyl)alkanes of the class R′CTp^{3-R} (R′ = Me, Et, *n*Pr, iBu; R = Et, *cy*Pr, Cy, *p-t*BuPh, Ph; *cy*Pr = cyclopropyl, Cy = cyclohexyl, *p-t*BuPh = *para-tert*-butylphenyl) were synthesised and their reactivity towards Mg(AlMe₄)₂ was examined. Along with new examples of recurring structural motifs, such as separated ion pairs and "metal in a box" complexes, *e.g.*, [(MeCTp^{3-Et})₂Mg][AlMe₄]₂, several magnesium complexes with new structural features/compositions were obtained. Treatment of the "metal in a box" species [(MeCTp^{3-R})Mg][AlMe₄]₂ with THF donor gave the terminal methyl complex [(MeCTp^{3-cyPr})MgMe(thf)₂][AlMe₄]. Variation of the backbone alkyl substituent R′ in the tris(pyrazolyl)alkane R′CTp^{3-Ph} gave ionic liquids (R′ = Et, *n*Pr) and the methyl-bridged dimagnesium complex [({iBuCTp^{3-Ph}}Mg{AlMe₄})₂(μ-Me)][AlMe₄]. The bulky Cy and *p-t*BuPh moieties at the pyrazolyl 3 position gave the new structural motif [MeCTp^{3-R}Mg(η^n-AlMe₄)][AlMe₄] (η^3, R = Cy; η^2, R = *p-t*BuPh), stabilising a "[Mg(AlMe₄)]$^+$" entity. The AlMe₃ group can be reversibly displaced under reduced pressure affording the new separated ion pair [(MeCTp$^{3-p-tBuPh}$)MgMe][AlMe₄] with a terminal "[MgMe]$^+$" moiety. Moderate thermal treatment of both [(MeCTp$^{3-p-tBuPh}$)MgMe][AlMe₄] and [(MeCTp$^{3-p-tBuPh}$)Mg(η^2-AlMe₄)][AlMe₄] resulted in selective C−H-bond activation in the 5 position of one of the pyrazolyl moieties and the formation of an AlMe₃-modified anionic tris(pyrazolyl)alkane and hence the neutral complex [MeC(pz$^{3-p-tBuPh}$)₂(pz$^{3-p-tBuPh,5-AlMe_3}$)]MgMe.

Introduction

While Grignard compounds RMgX (R = hydrocarbyl; X = Br, Cl) are among the most eminent reagents in organic synthesis,[1–8] the elucidation of the Schlenk equilibrium has clearly opened new avenues in organometallic chemistry. Crucially, manipulation of the Schlenk equilibrium by donor solvents features a viable path to dialkyl and diaryl magnesium species.[9,10] As early as 1964 Weiß structurally characterised [MgMe₂]$_n$, which was obtained in this way.[11] Since then, several donor-stabilised monomeric and dimeric complexes of [MgMe₂]$_n$ have been reported (*e.g.*, donor = quinuclidine, THF, TMEDA).[12–17]
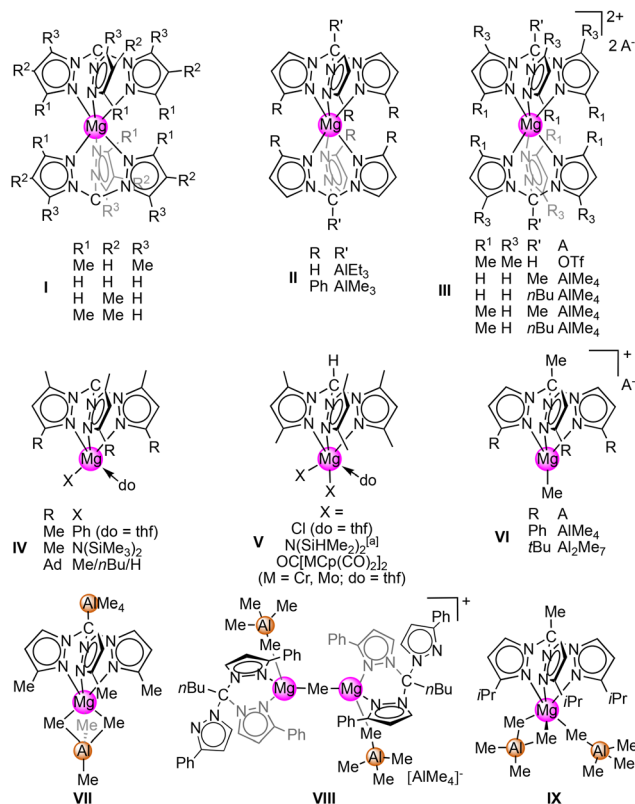
The seminal discoveries of tris(pyrazolyl)methane (HCTp) by Hückel und Bretschneider in 1935 (ref. 18) and subsequently of the trispyrazolylborato (Tp) scorpionate ligands in 1966 by Trofimenko paved the way for a new class of highly versatile ancillary ligands applicable in various areas of coordination chemistry.[19–27] Such polypyrazolyl scorpionate ligands

can be easily modified both at the pyrazole carbon atoms (Tp$^{3-R,5-R}$) and in the case of HCTp additionally at the apical carbon atom (R′CTp$^{3-R,4-R,5-R}$). Neutral R′CTp (R = H, alkyls) have been repeatedly used to stabilise highly reactive magnesium alkyl species.[28] Also, several complexes of magnesium bearing a mono-anionic CTp ligand have been structurally characterised (see Scheme 1).[29–34] "Metal in a box" complexes such as (CTp$^{3-R,4-R,5-R}$)₂Mg (**I**) were first described by Mountford and Breher in 2008.[29] Here, the application of magnesium dialkyl species led to the deprotonation of the backbone hydrogen. Similarly, such carbanion formation can be triggered in the presence of highly basic [AlMe₄] moieties, which can subsequently form trialkylaluminium adducts (or heteroaluminato-type species) to afford complexes (R₃AlCTp^{3-R})₂Mg (**II**).[30,35] By using an alkylated backbone or by protonating the apical carbanion with HOTf, separated ion pair "metal in a box" complexes [(R′CTp$^{3-R,5-R}$)₂Mg][A]₂ (**III**, A = OTf, AlMe₄) can be obtained.[29,35–37] When HCTp is reacted with a bulky magnesium base MgR₂ (R = Ph or [N(SiMe₃)₂]) or has a bulky substituent at the 3 position (adamantyl), deprotonation occurs as well but only one monoanionic CTp ligand coordinates at the magnesium centre to yield (CTp$^{3-Me,5-R}$)MgR (do) (**IV**).[29,30,34,35] Re-protonation of complexes of the type **IV** afforded (HCTp^{Me,Me})MgX₂(do) (**V**) with the neutral HCTp donor.[29,30,32]

Institut für Anorganische Chemie, Eberhard Karls Universität Tübingen (EKUT), Auf der Morgenstelle 18, 72076, Germany. E-mail: reiner.anwander@uni-tuebingen.de

Scheme 1 Structural motifs of reported magnesium tris(pyrazolyl) alkane and methanide complexes[a] κ^2(N,N′).

We have recently reported on several new magnesium tris (pyrazolyl)alkane complexes that resulted from the treatment of homoleptic tetramethylaluminate Mg(AlMe$_4$)$_2$ with differently substituted R′CTp^{3-R}.[35] The isolated complexes revealed species of types **II** and **III** as recurring structural motifs. Sterically demanding MeCTp^{3-R} (R = *t*Bu, Ph) ligands were able to stabilise a [MgMe]$^+$ fragment in compounds [(MeCTp^{3-R}) MgMe][A] (**VI**, A = AlMe$_4$, Al$_2$Me$_7$). Use of silyl-substituted Me$_3$SiCTp resulted in SiMe$_4$ elimination and formation of a monoanionic heteroaluminate species "Me$_3$AlCTp". Accordingly, a "metal in a box" complex could be prevented and the neutral Me$_3$AlCTp^{3-Me}Mg(AlMe$_4$) (**VII**) was isolated with one [AlMe$_4$] unit remaining at the magnesium centre. Longer alkyl chains in the backbone led to the dimagnesium complex [({*n*BuCTp^{3-Ph}}Mg{AlMe$_4$})$_2$(μ-Me)][AlMe$_4$] (**VIII**) with the rare κ^2(N,N′) coordination mode of the RCTp ligand. Finally, the MeCTp^{3-iPr} ligand provided the appropriate steric bulk to accommodate two [AlMe$_4$] units at the magnesium centre, namely MeCTp^{3-iPr}Mg(AlMe$_4$)$_2$ (**IX**).[35]
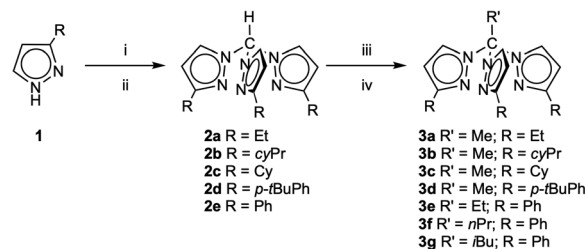
In the present study, we further expanded the tris(pyrazolyl)alkane ligand library [R′CTp^{3-R}] to gain an even better understanding of the steric influence of both the position 3 substituents on the pyrazolyl groups and the apical carbon atom substitution on the stabilisation of magnesium alkyl fragments.

Results and discussion

R′CTp^{3-R} ligand synthesis

Several new R′CTp^{3-R} derivatives were synthesized to investigate the feasibility of additional bis(aluminate) complexes of the favoured type **IX** (Scheme 1). The HCTp^{3-R} derivatives **2** were obtained from the corresponding 3-R-pyrazoles **1** applying the phase-transfer catalysis reaction of Elguero *et al.*, which was optimised by Reger *et al.*[38,39] To separate the desired product from the three other formed isomers, the mixture was refluxed with *p*-toluenesulfonic acid (Scheme 2). The apical carbon atom was alkylated in a one-pot synthesis by initial lithiation of the carbon atom with Li[N(SiMe$_3$)$_2$], followed by the addition of alkyl halides, which gives the neutral tris(pyrazolyl)alkane R′CTp^{3-R} (**3**, Scheme 2 and Fig. 1).

Considering the successful formation of the donor-stabilised bis(tetramethyl)aluminate magnesium complex **IX** employing MeCTp^{3-iPr}, tris(pyrazolyl)alkanes **3a–c** were synthesised to examine the steric demand of pyrazolyl substituents (R = Et, *cy*Pr, Cy) comparable to the iPr group and to complete the series of previously employed substituents Me and iPr.[35] The bulky **3d** (R = 3-*p*-tBuPh) was selected not only to prevent the formation of a "metal in a box" complex but also to assess the feasibility of methyl activation and hence the formation of a methylidene species. For comparison, the potassium salt of isoelectronic monoanionic Tp$^{3-p-tBuPh}$ formed the neutral complex Tp$^{3-p-tBuPh}$MgMe when reacted with MgMe$_2$.[40] We previously noticed a pronounced variability of the reactivity of monomeric Mg(AlMe$_4$)$_2$[41,42] towards R′CTp^{3-Ph} depending

Scheme 2 Preparation of ligands R′CTp^{3-R} **3a–g**. (i) (*n*Bu)$_4$NBr, CHCl$_3$, Na$_2$CO$_3$, H$_2$O, reflux, 3–7 d. (ii) *p*TsOH, toluene, 120 °C, 1 d. (iii) Li[N(SiMe$_3$)$_2$], THF, −78 °C, 30 min. (iv) RI, THF, −78 °C to rt, 16 h.
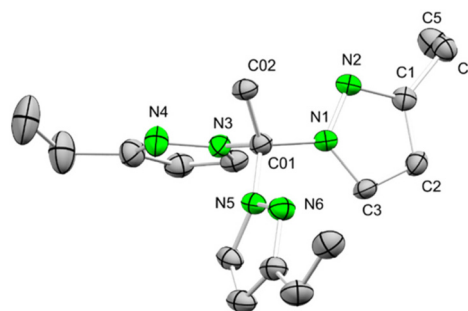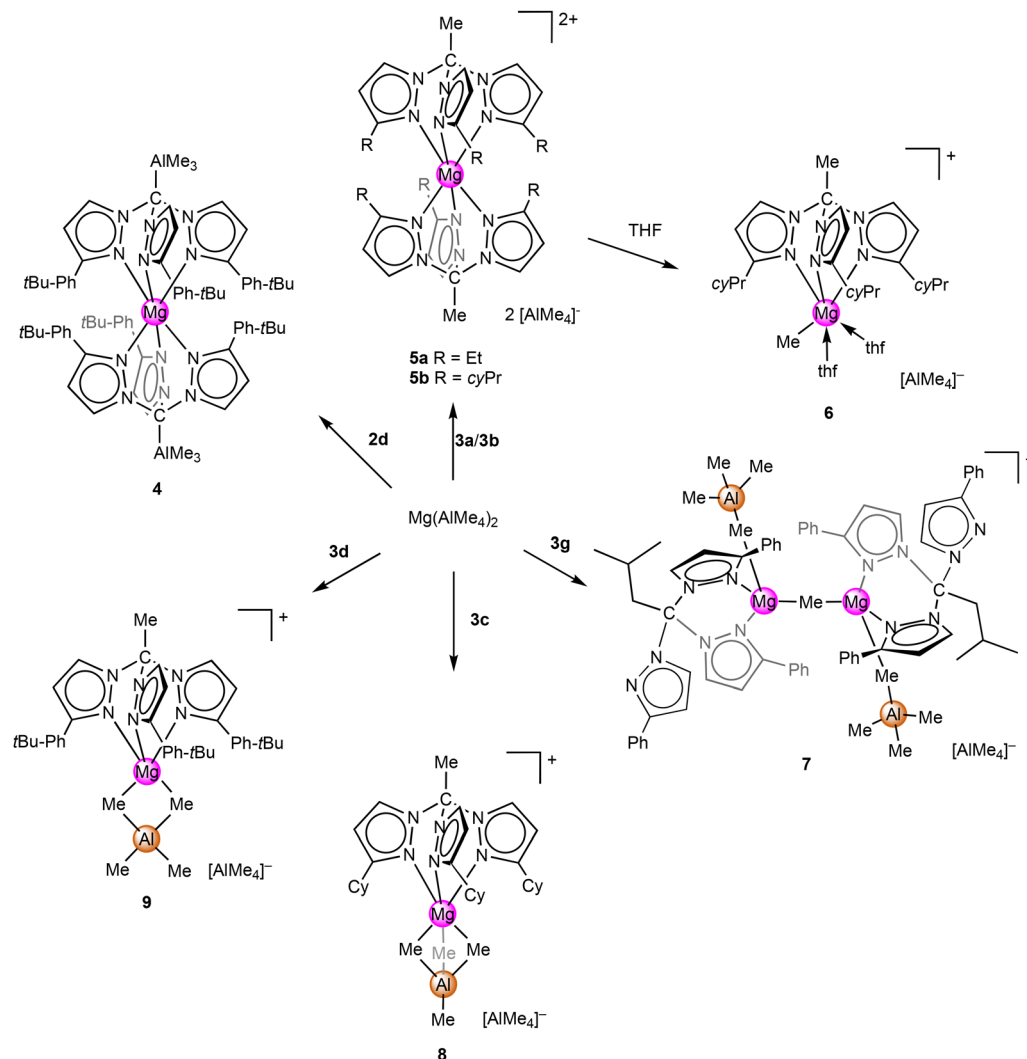

Fig. 1 Representative solid-state structure of **3a**. For the crystal structures of compounds **3b**, **3c** (connectivity) and **3e–g**, see the ESI.†

Scheme 3 Reaction of Mg(AlMe$_4$)$_2$ with **2d**, **3a–d** and **3g** in a toluene/*n*-hexane mixture.

on the chain length of R′, affording either separated ion pairs **VI** or the unusual methyl-bridged dimagnesium complex **VIII**. To further examine the effect of distinct backbone alkylation, the tris(pyrazolyl)alkanes **3e–g** (R′ = Et, *n*Pr, iBu) were targeted. All ligands were purified by recrystallization or column chromatography. Solid-state structures for **3a–c** and **3e–g** could be determined by single-crystal X-ray diffraction (SCXRD) analysis (Fig. 1 or ESI†). Tris(pyrazolyl)alkane backbone moieties other than alkyl chains (*e.g.* H, SiMe$_3$ or Bn = benzyl) were ruled out since we found previously that their reaction with Mg(AlMe$_4$)$_2$ either led to decomposition or carbanion formation *via* the displacement of the hydrogen atom at the apical carbon atom with an AlMe$_3$ moiety.

Magnesium R′CTp^{3-R} complexes

Homoleptic Mg(AlMe$_4$)$_2$ was previously identified as a suitable precursor preventing the decomposition of R′CTp^{3-R} ligands as observed in the case of MgMe$_2$.[35] For the synthesis of the new discrete magnesium complexes, a solution of Mg(AlMe$_4$)$_2$ in

n-hexane was added dropwise to a solution of **2d** or **3a–g** in toluene (for an overview see Scheme 3).

To assess whether the sterically demanding HCTp$^{3\text{-}p\text{-}t\text{BuPh}}$ (**2d**) can prevent methanide formation and any concomitant functionalization of the apical carbon atom, Mg(AlMe$_4$)$_2$ was treated with the crude product of **2d**. However, SCXRD analysis of the crystallized product revealed the recurring structural motif of the neutral "metal in a box" bis(methanide) complex (Me$_3$AlCTp$^{3\text{-}p\text{-}t\text{BuPh}}$)$_2$Mg (**4**) (see the ESI†). Even the bulky *p*-*t*BuPh groups protrude into the coordination sphere of the other scorpionate ligand and thus cannot prevent the accommodation of two monoanionic heteroaluminato ligands. The magnesium centre in **4** is coordinated by the six nitrogen atoms of the two methanide ligands in a distorted octahedral fashion with N–Mg–N angles in the range of 85.45(9) to 102.49 (14)°. The apical carbon–magnesium–apical carbon axis is close to linear (178.58°).

Treatment of Mg(AlMe$_4$)$_2$ with **3a/b** instantly gave a white precipitate indicative of the formation of a separated ion pair

with a "metal in a box" structure. This very structural motif could be confirmed by the solid-state structure of complex $[(MeCTp^{3-Et})_2Mg][AlMe_4]_2$ (**5a**) (Fig. 2). Two MeCTp^{3-Et} ligands coordinate the magnesium centre in the $\kappa^3(N,N',N'')$ mode forming a dicationic entity with two $[AlMe_4]^-$ anions as counter ions. The six-coordinated magnesium centre adopts a slightly distorted octahedral geometry with longer distances to the equatorial nitrogen atoms (Mg1–N2, 2.1666(10) Å; Mg1–N4, 2.1676(10) Å; Mg1–N6, 2.1458(10) Å). All observed Mg–N distances are in the expected range of magnesium complexes bearing two tris(pyrazolyl)methane ligands (2.113(1)–2.196(1) Å).[29–31,33,35] The CH$_2$ groups of the ethyl moiety are almost co-planar with the magnesium centre and the CH$_3$ groups are displaced only marginally from this plane. The apical carbon atom (C01) adopts an almost ideal tetrahedral geometry (109.21(9)–109.93(9)°). The NMR spectra of **5a** match those found in the reference literature, with ligand signals only slightly shifted.

In the ^{13}C NMR spectrum, the two $[AlMe_4]^-$ ions appear as a non-binominal sextet at $\delta = -4.2$ ppm due to the interaction with the ^{27}Al nucleus ($I = 5/2$, ^1J(Al,C) = 70.4 Hz) (Fig. S29†).[43] In the ^{1}H NMR spectrum, the proton signals of the $[AlMe_4]^-$ moieties appear at $\delta = -1.28$ ppm but the expected sextet is not fully resolved (Fig. S28†).

Given the similar reaction behaviour of the Mg(AlMe$_4$)$_2$/**3b** mixture involving product precipitation, the formation of putative complex $[(MeCTp^{3-cyPr})_2Mg][AlMe_4]_2$ (**5b**) seemed obvious. However, a crystalline material could only be obtained by heating a solid sample in a J. Young valve NMR tube to 150 °C in toluene. The structural motif of a separated ion pair
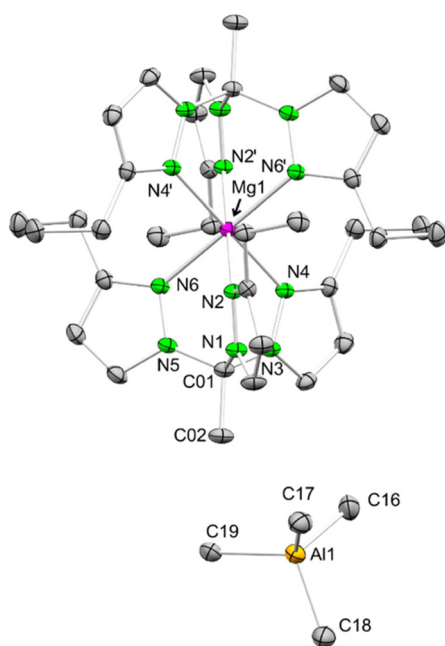
$[(MeCTp^{3-cyPr})_2Mg][AlMe_4]_2$ could be confirmed by a connectivity structure of crystals obtained under these harsh conditions (Fig. S6†). The formation of the "metal in a box" complex came as a surprise since the steric difference of cyPr and iPr is marginal. It is likely that the conformational/rotational flexibility of the iPr methyl moieties counteracts the coordination of a second MeCTp ligand. Because of the high insolubility of the precipitated product in aliphatic and aromatic solvents, THF was used as a solvent for NMR measurements. The ^{1}H NMR spectrum indicated that the separated ion pair converted to a complex of the type $[(MeCTp^{3-R})MgMe(thf)_2][AlMe_4]$ as proposed previously by NMR spectroscopy.[35] Crystallisation could be achieved by cooling the THF solution to −40 °C revealing the solid-state structure of methyl complex $[MeCTp^{3-cyPr}MgMe(thf)_2][AlMe_4]$ (**6**) (Fig. 3). The $[MgMe]^+$ fragment is coordinated by one MeCTp^{3-cyPr} ligand and two THF donor molecules, which are fully separated from the charge-balancing $[AlMe_4]^-$ counter ion. The magnesium centre adopts a distorted octahedral geometry with angles ranging from 78.18(10) to 105.39(17)°.

Unsurprisingly, the Mg1–C001 distance of 2.182(4) Å is slightly longer than those of 4-coordinate terminal methyl magnesium complexes $[MeCTp^{3-R}MgMe][AlMe_4]$ (R = tBu: 2.115(2) Å and R = Ph: 2.091(2) Å) and Tp^{R,Me}MgMe (R = Me: 2.097(4) Å and R = tBu: 2.119(3) Å) but distinctly shorter than the Mg–C distance involving the bridging position of MgMe$_2$ with 2.234(2) and 2.24(3) Å.[11,35,44,45] However, the Mg1–C001 distance in **6** is in line with other six-coordinate terminal methyl complexes $[MeMg(15-crown-5)][A]$ (A = Me$_5$Mg$_2$: 2.140(7) Å and A = Cp: 2.124(2) Å) and $[MeMg(thf)(dme)_2]I$ (2.162(6) Å).[46–48] It appears that the cyPr substituents of **6** provide enough steric flexibility so that the magnesium centre can accommodate two THF molecules, which is in contrast to complexes $[MeCTp^{3-R}MgMe][AlMe_4]$ (**VI**; R = tBu, Ph) mentioned above, in which the THF solvent is not coordinated to magnesium.

Fig. 2 Crystal structure of **5a**. Hydrogen atoms, one lattice THF molecule and the second $[AlMe_4]^-$ are omitted for clarity and atomic displacements are set at a 50% probability level.
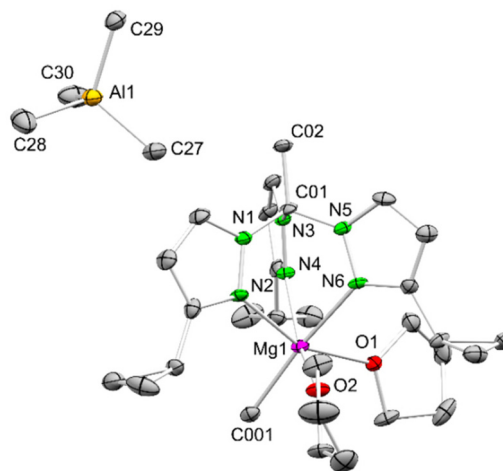

Fig. 3 Crystal structure of **6**. Hydrogen atoms are omitted for clarity and atomic displacements are set at a 50% probability level.

For further probing the impact of the apical carbon substitution, $Mg(AlMe_4)_2$ was reacted with R′CTp^{3-Ph} (R′ = Et (**3e**), *n*Pr (**3f**), and iBu (**3g**)). Note that complexes [MeCTp^{3-Ph}MgMe] [AlMe$_4$] (R′ = Me, type **VI**) and [({*n*BuCTp^{3-Ph}}Mg{AlMe$_4$})$_2$(μ-Me)][AlMe$_4$] (R′ = *n*Bu, **VIII**) were identified previously.[35] Accordingly, instant oil formation was observed in the case of tris(pyrazolyl)alkanes **3e** and **3f**. The crude products showed characteristic behaviour of an ionic liquid, impeding their crystallographic characterization. Moreover, the ^{1}H NMR spectra showed broadened signals that were not indicative of any structural motif detected so far. However, the $Mg(AlMe_4)_2$/**3g** reaction produced colourless crystals suitable for SCXRD analysis. The connectivity structure revealed that the methyl-bridged dimagnesium complex [({iBuCTp^{3-Ph}}Mg{AlMe$_4$})$_2$(μ-Me)][AlMe$_4$] (**7**, Fig. S8†) is isostructural to the previously identified *n*-butyl derivative **VIII**.

Further increasing the steric demand of the substituent in the 3 position of the pyrazole rings (compared to R′ = iPr, compound **IX**), $Mg(AlMe_4)_2$ was reacted with **3c** bearing cyclohexyl (Cy) groups. Crystals suitable for SCXRD analysis were obtained by recrystallisation in 1,2-difluorobenzene. The solid-state structure revealed the new structural motif of the separated ion pair [(MeCTp^{3-Cy})Mg(AlMe$_4$)][AlMe$_4$] (**8**) (Fig. 4).

The MeCTp^{3-Cy} ligand stabilises a [Mg(AlMe$_4$)]$^+$ fragment *via* κ^3(N,N′,N″) coordination while the [AlMe$_4$] ligand interacts with the magnesium centre in an η^3 fashion. The monoanionic [AlMe$_4$] counter ion is fully separated. The magnesium centre adopts a slightly distorted octahedral geometry with both ligands coordinating in a facial manner. The C01–Mg1–Al1 axis running through the ligand backbone is almost linear (176.45°). As expected the cyclohexyl groups adopt the chair conformation pointing away from the magnesium centre just like the *cy*Pr groups in **6** and the iPr groups in **IX**.[35]

Crystallisation of the reaction product formed by the treatment of $Mg(AlMe_4)_2$ with the bulky **3d** (with R′ = *p*-*t*BuPh) was achieved by redissolving the residue in benzene and dropwise addition of *n*-pentane to the solution at 40 °C. As detected for **8**, the solid-state structure revealed the formation of a monocationic complex entity in [(MeCTp$^{3-p-tBuPh}$)Mg(AlMe$_4$)][AlMe$_4$] (**9**) (Fig. 5) with the magnesium centre also coordinated with one tris(pyrazolyl)ethane ligand in the κ^3(N,N′,N″) mode. However, due to the enhanced steric demand of **3d** compared to **3c**, this time the [AlMe$_4$] unit is η^2-coordinated. The now 5-coordinate magnesium centre adopts a strongly distorted square pyramidal geometry with two nitrogen atoms (N2 and N4) of the scorpionate ligand and two carbon atoms of the [AlMe$_4$] unit (C40 and C41) located in the equatorial and one ligand nitrogen (N6, the "sting") in the apical position. Hence, the coordination of the MeCTp$^{3-p-tBuPh}$ ligand itself appears highly asymmetrical, very much scorpionate-like with two pincers and one sting. The putative sixth coordination position for octahedral geometry is approached by *ortho*-carbon atoms of two different phenyl rings (C18: 3.592, C9: 3.700 Å). The overall asymmetric coordination of the scorpionate ligand is also seen in the distance of the phenyl rings, measured by the distance of the *ortho*-carbon atoms closest to each other (C9–C18 4.118 Å, C5–C31 6.187 Å, and C22–C35 8.567 Å) and furthermore in the N–N distances between the three coordinating nitrogen atoms (N2–N4 2.717 Å, N2–N6 2.877 Å, and N4–N6 3.110 Å), as well as by the N–Mg–N angles (N2–Mg1–N4 76.64(5)°, N2–Mg1–N6 83.24(6)°, and N4–Mg1–N6 91.91(6)°). Finally, the C01–Mg1–Al1 axis deviates considerably from linearity (165.43°).

The pronounced asymmetric tris(pyrazolyl)ethane coordination in complex **9** is not detected in the ambient tempera-
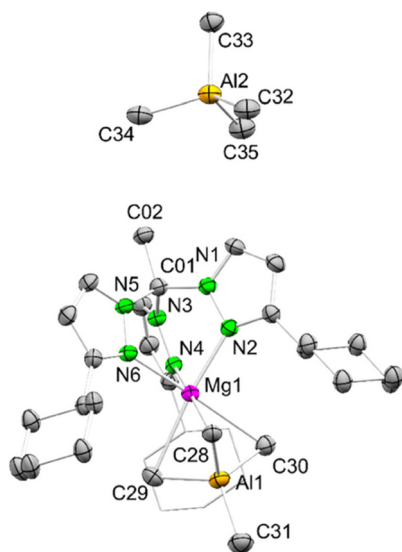

Fig. 4 Crystal structure of **8**. Hydrogen atoms are omitted for clarity and atomic displacements are set at a 50% probability level.

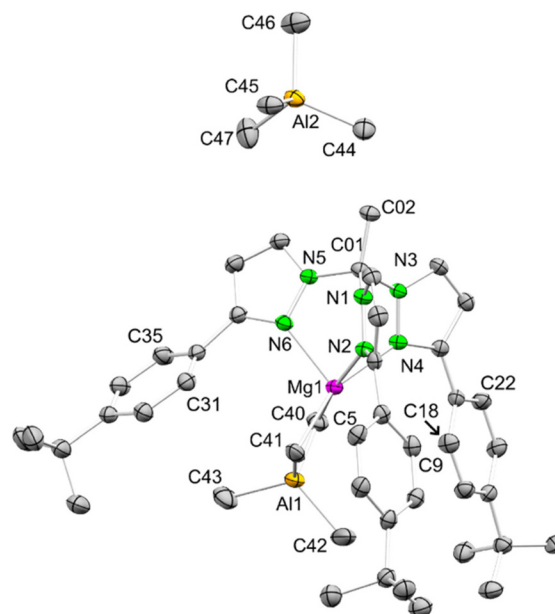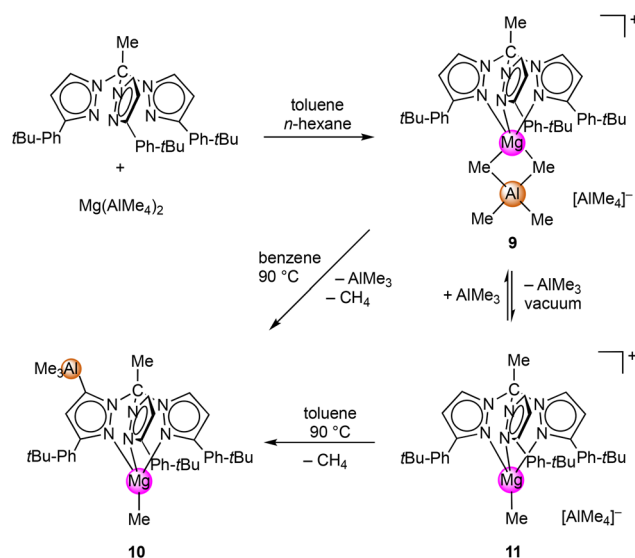**Fig. 5** Crystal structure of **9**. Hydrogen atoms, the lattice [D$_6$]benzene molecules and the disorder in one *t*Bu group are omitted for clarity and atomic displacements are set at a 50% probability level.

ture ^{1}H NMR spectrum, which is similar to that of complex **8**. The two pyrazole hydrogen atoms in the 4- and 5 positions appear as multiplets in the aromatic region at $\delta = 8.03/7.84$ ppm and $\delta = 6.28/5.80$ ppm, respectively, with an integral of each being three. Also, there is only one sharp signal found for the bridging and terminal methyl groups of the co-ordinated [AlMe$_4$] unit and for the methyl groups of the displaced [AlMe$_4$] at $\delta = -0.19$ (**8**)/-0.34 ppm (**9**), which indicates fast exchange of the coordinated and free tetramethyl-aluminato groups. Because of this dynamic behaviour VT ^{1}H NMR spectroscopy experiments were performed on both complexes **8** and **9** (Fig. S34/38†). Accordingly, the signals at $\delta = -0.19$ ppm and $\delta = -0.34$ ppm broaden as the temperature decreases. For **8**, the signal splits into two separated singlets at $-50\ °C$ while for **9** this behaviour is detected at $-60\ °C$. At $-80\ °C$, these two signals are located at $\delta = 0.18$ and -0.06 ppm (**8**) and at $\delta = 0.24$ and -0.79 ppm (**9**), both in a ratio of $2:1$. All other signals ascribed to **8** split into two signals at $-80\ °C$ even that of the backbone methyl group, which means that the [AlMe$_4$] group exchange is more complicated. The same signal splitting is observed for **9** (at $-80\ °C$) except that the signal of the backbone methyl group appears as a very broad signal. This could indicate that for **9** only one R′CTp^{3-R} ligand species is present during the exchange of the [AlMe$_4$] groups, but acts in a hemilabile fashion with one arm off. The splitting of the signals is completely reversible for both complexes upon warming the solutions to ambient temperatures. Complex **9** also remains intact when heated to 80 °C and re-cooled to ambient temperature.

Behaviour of [(MeCTp$^{3-p-tBuPh}$)Mg(AlMe$_4$)][AlMe$_4$] (9) at elevated temperatures and under vacuum

As revealed by ^{1}H NMR spectroscopy, further heating of complex **9** to 90 °C led to a selective activation of the scorpio-nate ancillary ligand. Full conversion was indicated by a new set of signals showing the pyrazolyl moieties in a ratio of $1:2$ along with the backbone methyl group, which appeared slightly shifted to lower field. Slow evaporation of the solvent generated crystals suitable for SCXRD analysis. The solid-state structure revealed C–H-bond activation of one pyrazole ring at the 5 position forming the neutral complex [MeC(pz$^{3-p-tBuPh}$)$_2$(pz$^{3-p-tBuPh,5-AlMe_3}$)]MgMe (**10**) (Scheme 4 and Fig. 6). Notably, heating a solution of **10** to 100 °C resulted in complete decomposition. Complex **10** adopts a distorted tetrahedral geo-metry with the magnesium centre accommodating the new scorpionate ligand in the routine η^3 fashion and a terminal methyl group. The Mg1–C43 distance of 2.090(2) Å matches other terminal Mg–C distances of tetrahedral magnesium methyl complexes.[35,44] Due to the metalation of one pyrazolyl ring the scorpionate ligand is monoanionic. Because of this and the less bulkier methyl group the overall geometry of the ligand scaffold is more symmetrical in comparison with that of complex **9**. As a consequence, the N–N distances of the three coordinating nitrogen atoms lie between 2.842 and 2.873 Å (cf., **9** $\Delta_{max} = 0.393$ Å) and the C01–Mg1–C43 axis is close to linear (177.65°). Since the scorpionate ligand in **10** is

Scheme 4 Thermal activation and reversible coordination of AlMe$_3$ in complex **9**. R = *p*-tBuPh.

Fig. 6 Crystal structure of **10**. Hydrogen atoms and two solvent toluene molecules are omitted for clarity and atomic displacements are set at a 50% probability level.

monoanionic, complex **10** is now comparable to the Tp$^{3-p-tBuPh}$MgMe complex proposed by Parkin.[40] A striking feature of the ^{1}H NMR spectrum of **10** is the considerable low-field shift at $\delta = 7.32$ ppm of the singlet of the hydrogen atom in the 4 position of the activated pyrazolyl ring. In contrast, the doublet signal of the hydrogen atom in the 4 position of the non-activated pyrazolyl rings appears at $\delta = 5.90$ ppm. The methyl ligand and the AlMe$_3$ group were detected at $\delta = -0.99$ ppm and 0.16 ppm, respectively.

By applying reduced pressure, AlMe$_3$ can be displaced from complex **9** forming the new separated ion pair [(MeCTp$^{3-p-tBuPh}$)MgMe][AlMe$_4$] (**11**) (Scheme 4). The ^{1}H NMR spectrum of **11** shows slightly shifted signals of the ancillary ligand while the counter ion [AlMe$_4$] and the methyl group co-

ordinated to the magnesium centre appear as two distinct signals at δ = −0.09 ppm and −1.04 ppm, respectively (Fig. S42†). Adding a stoichiometric amount of AlMe$_3$ to **11** reformed complex **9** quantitatively, thus proving full reversibility. This behaviour is reminiscent of the Tp^{Me,Me}Mg(AlMe$_4$)/ Tp^{Me,Me}MgMe system engaging in donor-induced tetraalkylaluminate cleavage.[42] Heating complex **11** to 90 °C also led to the formation of complex **10**, suggesting that the C–H-bond activation in the 5 position of the pyrazolyl moiety is caused by the attack of the separated [AlMe$_4$] anion *via* the release of methane.

Cone angle calculations

The mathematically exactly calculated cone angles[49] of the scorpionate ligands of the newly synthesised complexes are shown in Table 1. The cone angles featured by [(MeCTp^{3-Et})$_2$Mg][AlMe$_4$]$_2$ (**5a**, $\Theta°$ = 247.95°) and [MeCTp^{3-cyPr}MgMe(thf)$_2$][AlMe$_4$] (**6**, $\Theta°$ = 250.80°) are very close to that observed for the bis(tetramethylaluminato) complex [(MeCTp^{3-iPr})Mg(AlMe$_4$)$_2$] (Θ = 248.76°).[35] Despite this similarity, completely different coordination environments exist even though all complexes exhibit a coordination number of six. It seems that the slightly higher steric demand of the iPr group in comparison to Et and cyPr, caused by the flexibility of the two Me groups, is sufficient to prevent the formation of the "metal in a box" complex. As expected the cone angle calculated for [(MeCTp^{3-Cy})Mg(AlMe$_4$)][AlMe$_4$] (**8**) ($\Theta°$ = 260.64°) is distinctly higher than that enforced by the iPr, Et or cyPr substituents, which allows the stabilization of the Mg(η^3-AlMe$_4$)$^+$ fragment with three methyl groups coordinated to the metal centre. The tentative cone angles of the two disordered species of **9** are determined as $\Theta°$ = 289.60° and $\Theta°$ = 291.34°. The only magnesium complexes with a cone angle comparable to **9** are [(MeCTp^{3-Ph})MgMe][AlMe$_4$] ($\Theta°$ = 282.84°) and the extremely bulky [(CTp^{Ad,Me})MgMe] ($\Theta°$ = 301.47°).[35,50] Upon thermal C–H-bond activation and formation of [MeC (pz$^{3-p-tBuPh}$)$_2$(pz$^{3-p-tBuPh,5-AlMe_3}$)]MgMe (**10**), the cone angle increased even further to $\Theta°$ = 299.10°. Now that the scorpionate ligand has a negative charge it is better comparable to the adamantyl methanide complex [(CTp^{Ad,Me})MgMe] and both angles are indeed very close. Comparing the cone angles of (Me$_3$AlCTp$^{3-p-tBuPh}$)$_2$Mg (**4**) and **10**, which both feature anionic scorpionate ligands with p-tBuPh moieties in the 3 position, there is a difference of 11.08°. Therefore, the ligand coordinated to the metal centre opposite to the examined/calculated R′CTp^{3-R} ligand has a vast influence on the cone angle too.

Table 1 Overview of the mathematically exactly calculated cone angle $\Theta°$ of the magnesium tris(pyrazolyl)alkane complexes under study (see the ESI† for calculations)

4	5a	6	8	9	10
288.02	247.95	250.80	260.64	289.60	299.10
				291.34	

Conclusions

The scope of the tris(pyrazolyl)alkane R′CTp^{3-R} library, here with varying substituents in the pyrazolyl 3 position and at the apical carbon atom, could be successfully expanded by derivatives MeCTp^{3-Et}, MeCTp^{3-cyPr}, MeCTp^{3-Cy}, MeCTp$^{3-p-tBuPh}$, EtCTp^{3-Ph}, nPrCTp^{3-Ph} and iBuCTp^{3-Ph} (cyPr = cyclopropyl, Cy = cyclohexyl, 3-p-tBuPh = *para-tert*-butylphenyl). As anticipated, the reaction of bis(tetramethylaluminato) magnesium Mg(AlMe$_4$)$_2$ with neutral tris(pyrazolyl)alkanes R′CTp^{3-R} is strongly dependent on the steric effect of such scorpionate ligands, resulting in the partial or full displacement of the aluminato ligands. The smaller Et and cyPr substituents in the 3 position favour the formation of the recurring "undesired" structural motifs of a "metal in a box" complex [(MeCTp^{3-R})$_2$Mg][AlMe$_4$]$_2$ (R = Et, cyPr). The bulky Cy and p-tBuPh moieties led to the separated ion pairs [(MeCTp^{3-R})Mg (AlMe$_4$)][AlMe$_4$] (R = Cy, p-tBuPh) with distinct η^2- and η^3- coordination modes of the AlMe$_4$ moiety. Variation of the alkyl substituent R′ at the apical carbon atom of R′CTp^{3-Ph} (R′ = Et, nPr, iBu) led to the isolation of the dimagnesium species [({iBuCTp^{3-Ph}}Mg{AlMe$_4$})$_2$(μ-Me)][AlMe$_4$] with a κ^2(N,N′) coordination mode of the tris(pyrazolyl)alkane ligand. Separated ion pairs of the type [(MeCTp^{3-R})Mg(AlMe$_4$)][AlMe$_4$] are prone to AlMe$_3$ separation, when exposed to a vacuum, and a selective pyrazolyl deprotonation, upon thermal treatment. The latter C–H-bond activation is triggered by the non-coordinating [AlMe$_4$] anion and generates a new monoanionic scorpionate ligand in [MeC(pz$^{3-p-tBuPh}$)$_2$(pz$^{3-p-tBuPh,5-AlMe_3}$)]MgMe featuring a terminal Mg–CH$_3$ moiety.

Experimental

General considerations

All manipulations were performed under rigorous exclusion of air and moisture under an argon atmosphere (<1 ppm O$_2$, <1 ppm of H$_2$O) in an MB200B glovebox (MBraun) or according to standard Schlenk techniques and in oven-dried glassware. Solvents (THF, n-pentane, n-hexane, Et$_2$O and toluene) were purified by using Grubbs-type columns (MBraun SPS-800, solvent purification system) and stored inside a glovebox. THF was dried further over molecular sieves. [D$_6$]Benzene, [D$_8$] toluene and [D$_8$]THF were obtained from Sigma Aldrich and dried over a Na/K alloy and filtered prior to use. 1,4-Dioxane was dried over sodium metal, distilled and degassed and stored inside a glovebox. 1,2-Difluorobenzene was purchased from Sigma Aldrich, dried over CaH$_2$, distilled and degassed prior to use. Acetophenone (>98%), benzophenone (>98%), n-BuLi (2.5 M in n-hexane), cyclopropyl methyl ketone (99%), 1,4-dihydro-2H-pyrane (>97%), ethyl bromide (>99%), ethyl iodide (99%, copper stabilized), hexamethyldisilazane (>99%), hydrazine dihydrochloride (>98%), methylmagnesium bromide (3 M in Et$_2$O), n-propyl iodide (99%), 1-iodo-2-methyl-propane (97%, copper stabilized), pyrazole (>98%) and tetra-n-butylammonium bromide (98%) were purchased from Sigma

Aldrich and used as received. Iodomethane (>99%) and methyl *tert*-butyl ether (MTBE) were purchased from Acros Organics and used as received. *N,N*-Dimethylformamide dimethylacetate (>97%), 4′-*tert*-butylacetophenone (98%) and trimethylaluminium (98%) were purchased from abcr and used as received. Cyclohexyl methyl ketone (95%) was purchased from Alfa Aesar and used as received. $Li[N(SiMe_3)_2]$,[51] $MgMe_2$[9,10] and $Mg(AlMe_4)_2$[41] were synthesized according to the literature procedures. The 3-R-pyrazoles **1** were synthesized according to standard procedures (R = Et,[52] *cy*Pr,[53] Cy,[53] Ph,[53] *p-t*BuPh [53]). Argon was supplied by Westfalen AG. ^1H and ^{13}C NMR spectra were recorded on a Bruker AVII+400 spectrometer (^1H: 400.11 MHz; ^{13}C: 100.61 MHz) at 299 K. The chemical shifts compiled in the Experimental section are referenced to solvent residual resonances in parts per million relative to tetramethylsilane. The variable temperature ^1H NMR spectra of **8** and **9** were recorded in a J. Young valve NMR tube on a Bruker AVII+500 spectrometer (^1H: 500.13 MHz; ^{13}C: 125.76 MHz) at 299 K. IR spectra were recorded on a NICOLET 6700 FTIR spectrometer (Thermo Fisher Scientific). The samples were mixed with KBr powder and measured in a DRIFT cell with KBr windows. DRIFT data were converted by using the Kubelka–Munk refinement. Elemental analyses were performed on an Elementar Vario MICRO cube. Single crystals were grown from saturated solutions of $[D_6]$benzene, 1,2-difluorobenzene, Et_2O, MTBE, *n*-pentane, or THF by standard techniques. Suitable single crystals for X-ray structure studies were selected in a glovebox and coated with Parabar 10312 (Hampton Research). Crystallographic data were measured on a Bruker APEX II DUO instrument equipped with an IμS micro focus sealed tube and QUAZAR optics for MoK_α radiation ($\lambda = 0.71073$ Å). The structures were solved by direct methods using SHELXT software packages and refined on F^2 (with all independent reflections) using the SHELXL software package. The non-hydrogen atoms were refined anisotropically. All hydrogen atoms of C–H bonds were located using a riding model at the expected position for hydrogen with a fixed interatomic distance.

General procedure for the synthesis of 2. The synthesis of tris(pyrazolyl)alkanes **2** was achieved according to the literature procedure by Reger.[39] In a 1 L three-necked flask with a KPG stirrer the corresponding 3-alkylpyrazole (1 equiv.), Na_2CO_3 (20 equiv.) and (*n*-Bu)$_4$NBr (0.05 equiv.) were dissolved in 350 mL each of water and $CHCl_3$. The reaction mixture was heated to 95 °C and was stirred vigorously until completeness (3–7 days). After cooling to ambient temperature, water was added to dissolve excess Na_2CO_3. The organic layer was separated and the solvent was removed under reduced pressure. After redissolving the residue in Et_2O and combining all layers the aqueous layer was washed three times with Et_2O. The combined organic layers were dried over Na_2SO_4, filtered and the solvent was removed under reduced pressure. The residual dark red oil was redissolved in 200 mL of toluene in a 500 mL round bottom flask. After adding 400 mg of *p*TsOH the mixture was heated to reflux for 1 d. After cooling to ambient temperature, the reaction mixture was washed with brine and the aqueous layer was extracted three times with Et_2O. The combined organic layers were dried with Na_2SO_4 and filtered. After removal of the solvent *in vacuo* an oil was obtained. Unreacted pyrazole could be separated by sublimation. The ^1H NMR spectra showed that the oil was a mixture of the desired product **2** ($HC(pz^{3-R})_3$) and the undesired isomer ($HC(pz^{3-R})_2(pz^{5-R})$) with one flipped pyrazolyl moiety. The isomer ratio depended on the steric bulk of the corresponding pyrazole and was determined by comparison of the backbone hydrogen H-CTp^{3-R} signal integrals. Used quantities and yields for **2**:

HCTp^{3-Et} (2a). 3-Ethylpyrazole (27.2 g, 282 mmol), Na_2CO_3 (180 g, 1.697 mol), and (*n*-Bu)$_4$NBr (4.56 g, 14 mmol). Reaction time: 7 d. **2a** was obtained as a dark red oil (88%, 24.7 g, 82.9 mmol). The ratio of the crude product mixture: **2a** : undesired isomer = 1 : 0.4.

HCTp^{3-cyPr} (2b). 3-Cyclopropylpyrazole (25.0 g, 231 mmol), Na_2CO_3 (143 g, 1.350 mol), and (*n*-Bu)$_4$NBr (3.62 g, 11 mmol). Reaction time: 7 d. **2b** was obtained as a dark brown oil (81%, 21.1 g, 63 mmol). The ratio of the crude product mixture: **2b** : undesired isomer = 1 : 0.6.

HCTp^{3-Cy} (2c). 3-Cyclohexylpyrazole (24.0 g, 160 mmol), Na_2CO_3 (102 g, 960 mmol), and (*n*-Bu)$_4$NBr (2.58 g, 8.0 mmol). Reaction time: 5 d. **2c** was obtained as a dark red oil in a quantitative yield. The ratio of the crude product mixture: **2c** : undesired isomer = 1 : 0.2.

HCTp$^{3-p-tBuPh}$ (2d). 3-*para-tert*-Butylphenylpyrazole (25.0 g, 124 mmol), Na_2CO_3 (79.4 g, 749 mol), and (*n*-Bu)$_4$NBr (2.0 g, 6.2 mmol). Reaction time: 7 d. **2d** was obtained as a dark red oil (50%, 11.4 g, 19 mmol). The ratio of the crude product mixture: **2d** : undesired isomer = 1 : 0.1.

HCTp^{3-Ph} (2e). 3-Phenylpyrazole (25.0 g, 173 mmol), Na_2CO_3 (110 g, 1.040 mol), and (*n*-Bu)$_4$NBr (2.80 g, 8.7 mmol). Reaction time: 3 d. **2e** was obtained as a dark red oil (45%, 11.5 g, 26 mmol). The ratio of the crude product mixture: **2e** : undesired isomer = 1 : 0.1.

Preparation and characterization of compounds 3, 4, 5, 6, 8, 9, 10 and 11

MeCTp^{3-Et} (3a). The crude product of HCTp^{3-Et} (**2a**) (3.00 g, 10.1 mmol) was dissolved in 80 mL of THF. After cooling to −78 °C, a solution of $Li[N(SiMe_3)_2]$ (2.52 g, 15.1 mmol) in THF was added dropwise. The reaction mixture was allowed to warm to ambient temperature and stirred for another hour. After re-cooling to −78 °C, MeI (0.94 mL, 15.1 mmol) was added dropwise and the mixture was allowed to warm to ambient temperature. After stirring at ambient temperature overnight, water (50 mL) was added, THF was removed under reduced pressure and the aqueous solution was extracted three times with Et_2O (50 mL). The combined organic layers were dried over Na_2SO_4, filtered and the solvent was removed under reduced pressure. The obtained dark red oil was chromatographed on a silica gel column that was packed and flushed with a mixture of 3 : 1 petroleum ether and Et_2O. The fractions containing the desired product were combined and the solvent was removed under reduced pressure, which gave **3a** as a colourless powder (670 mg, 2.14 mmol, 28%). Crystals suitable

for SCXRD analysis could be obtained by recrystallization from MTBE. ^{1}H NMR (400.1 MHz, CDCl$_3$, 26 °C): δ = 6.52 (d, 3H, $^3J_{HH}$ = 2.5 Hz; 5-H(pz)), 6.09 (d, 3H, $^3J_{HH}$ = 2.5 Hz; 4-H(pz)), 2.91 (s, 3H; CH_3CTp), 2.67 (q, 6H, $^3J_{HH}$ = 7.6 Hz; CH_2CH$_3$), 1.24 ppm (t, 3H, $^3J_{HH}$ = 7.6 Hz; CH$_2$CH_3). ^{13}C{^{1}H} NMR (100.6 MHz, CDCl$_3$, 26 °C): δ = 156.7 (3-C(pz)), 129.6 (5-C(pz)), 104.8 (4-C(pz)), 90.1 (CH$_3$$C$Tp), 25.9 (CH$_3$CTp), 21.6 (CH$_2CH_3$), 13.8 ppm (CH$_2CH_3$). DRIFTS: $\tilde{\nu}_{max}$ = 3134w, 3115w, 2969s, 2935m, 2873m, 2641vw, 1703vw, 1526s, 1467m, 1454m, 1371s, 1312m, 1260s, 1209s, 1112m, 1049s, 1008w, 976m, 952w, 796s, 759s, 659w, 632w, 578vw, 439vw cm^{-1}. Elemental analysis calcd (%) for C$_{17}$H$_{24}$N$_6$ (312.42 g mol^{-1}): C 65.36, H 7.74, N 26.90; found: C 65.49, H 7.47, N 26.94.

MeCTp^{3-cyPr} (3b). Following the procedure described for **3a**, the crude product of **2b** (3.00 g, 8.89 mmol), Li[N(SiMe$_3$)$_2$] (1.95 g, 11.7 mmol) and MeI (1.50 mL, 11.2 mmol) yielded **3b** as a brownish oil as the crude product. Further purification was achieved by flash column chromatography with a 3 : 1 mixture of petroleum ether and Et$_2$O with subsequent recrystallization from Et$_2$O to afford **3b** as colourless crystals (983 mg, 2.82 mmol, 31%) suitable for SCXRD analysis. ^{1}H NMR (400.1 MHz, CDCl$_3$, 26 °C): δ = 6.46 (d, 3H, $^3J_{HH}$ = 2.6 Hz, 5-H(pz)), 5.85 (d, 3H, $^3J_{HH}$ = 2.6 Hz, 4-H(pz)), 2.84 (s, 3H, CH_3CTp), 1.92 (m, 3H, (CH$_2$)$_2$CH), 0.88 (m, 6H, (CH_2)$_2$CH), 0.67 ppm (m, 6H, (CH_2)$_2$CH). ^{13}C{^{1}H} NMR (100.6 MHz, CDCl$_3$, 26 °C): δ = 157.2 (3-C(pz)), 129.7 (5-C(pz)), 102.7 (4-C(pz)), 90.1 (CTp), 25.8 (CH$_3$CTp), 9.4 ((CH$_2$)$_2$CH), 8.2 ppm ((CH$_2$)$_2$CH). DRIFTS: $\tilde{\nu}_{max}$ = 3142w, 3124w, 3087vw, 3003m, 2952w, 2852vw, 2469vw, 2075vw, 1708w, 1613vw, 1531vs, 1480m, 1444m, 1397s, 1371s, 1305s, 1259vs, 1220s, 1208vs, 1177s, 1113m, 1045s, 988s, 883m, 763s, 709vw, 561vw, 631vw, 488vw cm^{-1}. Elemental analysis calcd (%) for C$_{20}$H$_{24}$N$_6$ (348.21 g mol^{-1}): C 68.94, H 6.94, N 24.12; found C 68.86, H 6.85, N 23.99.

MeCTp^{3-Cy} (3c). Following the procedure described for **3a**, the crude product of **2c** (2.65 g, 5.75 mmol), Li[N(SiMe$_3$)$_2$] (1.93 g, 11.5 mmol) and MeI (0.72 mL, 11.5 mmol) yielded a mixture of a dark red oil and small cubic crystals. After recrystallization from methyl *tert*-butyl ether and washing with MeOH, **3c** could be obtained as cubic colourless crystals (344 mg, 0.72 mmol, 13%). ^{1}H NMR (400.1 MHz, CDCl$_3$, 26 °C): δ = 6.39 (m, 3H; 5-H(pz)), 6.05 (m, 3H; 4-H(pz)), 2.90 (s, 3H; CH_3CTp), 2.68 (m, 3H; 1-H(Cy)), 1.96–1.94 (m, 6H; 2,6-H(Cy)), 1.80–1.77 (m, 6H; 3,5-H(Cy)), 1.73–1.69 (m, 3H; 4-H(Cy)), 1.45–1.31 (m, 12H; 2,6-; 3,5-H(Cy)), 1.30–1.20 ppm (m, 3H; 4-H(Cy)). ^{13}C{^{1}H} NMR (100.6 MHz, CDCl$_3$, 26 °C): δ = 160.3 (3-C(pz)), 129.4 (5-C(pz)), 103.4 (4-C(pz)), 90.3 (CH$_3$$C$Tp), 37.7 (1-$C$(Cy)), 33.2 (2,6-$C$(Cy)), 26.3 (3,5-$C$(Cy)), 26.1 (4-$C$(Cy)), 25.7 ppm (CH$_3$CTp). DRIFTS: $\tilde{\nu}_{max}$ = 2922s, 2849m, 1522m, 1447w, 1370w, 1347vw, 1289vw, 1260m, 1232w, 1213w, 1132vw, 1106vw, 1058w, 1033vw, 977w, 891vw, 817vw, 793m, 768w, 752m, 640vw cm^{-1}. Elemental analysis calcd (%) for C$_{29}$H$_{42}$N$_6$ (474.70 g mol^{-1}): C 73.38, H 8.92, N 17.70; found: C 73.23, H 8.73, N 17.42.

MeCTp$^{3-p-tBuPh}$ (3d). Following the procedure described for **3a**, the crude product of **2d** (2.00 g, 3.27 mmol), Li[N(SiMe$_3$)$_2$]

(822 mg, 4.91 mmol) and MeI (0.31 mL, 4.91 mmol) yielded a mixture of a dark red oil and a colourless solid. The solid was washed five times with *n*-pentane. Further purification was achieved by flash column chromatography with a 5 : 1 mixture of petroleum ether and Et$_2$O to afford **3d** as a colourless powder (671 mg, 10.7 mmol, 33%). ^{1}H NMR (400.1 MHz, CDCl$_3$, 26 °C): δ = 7.79 (m, 6H; *o*-H(Ph)), 7.45 (m, 6H; *m*-H(Ph)), 6.82 (d, 3H, $^3J_{HH}$ = 2.5 Hz; 5-H(pz)), 6.58 (d, 3H, $^3J_{HH}$ = 2.5 Hz; 4-H(pz)), 3.16 (s, 3H; CH_3CTp), 1.36 ppm (s, 27H; C(CH_3)$_3$). ^{13}C{^{1}H} NMR (100.6 MHz, CDCl$_3$, 26 °C): δ = 153.2 (3-C(pz)), 151.3 (*p*-C(Ph)), 130.5 (5-C(pz)), 130.1 (i-C(Ph)), 125.7 (*o*-C(Ph)), 125.5 (*m*-C(Ph)), 103.8 (4-C(pz)), 91.1 (MeCTp), 34.6 (C(CH$_3$)$_3$), 31.3 (C(CH$_3$)$_3$), 26.0 ppm (CH$_3$CTp). DRIFTS: $\tilde{\nu}_{max}$ = 3127vw, 2963m, 2902w, 2865w, 1719vw, 1668vw, 1605vw, 1501m, 1450w, 1387w, 1365m, 1268m, 1232s, 1124w, 1089vw, 1047w, 1017vw, 978vw, 948vw, 839m, 793m, 763m, 742w, 700vw, 642vw, 560w, 501vw cm^{-1}. Elemental analysis calcd (%) for C$_{41}$H$_{48}$N$_6$ (624.88 g mol^{-1}): C 78.81, H 7.74, N 13.45; found: C 79.01, H 7.85, N 13.35.

EtCTp^{3-Ph} (3e). Following the procedure described for **3a**, the crude product of **2e** (2.00 g, 4.52 mmol), Li[N(SiMe$_3$)$_2$] (983 mg, 5.88 mmol) and EtI (542 μL, 6.78 mmol) yielded **3e** as a pale yellow solid as the crude product. Further purification was achieved by recrystallization from a 1 : 1 mixture of *n*-hexane and MTBE to afford **3e** as colourless crystals (1.55 g, 3.28 mmol, 73%) suitable for SCXRD analysis. ^{1}H NMR (400.1 MHz, CDCl$_3$, 26 °C): δ = 7.86 (m, 6H, *o*-H(Ph)), 7.38 (m, 9H, *m*-H(Ph), *p*-H(Ph)), 7.07 (d, 3H, $^3J_{HH}$ = 2.8 Hz, 5-H(pz)), 6.62 (d, 3H, $^3J_{HH}$ = 2.7 Hz, 4-H(pz)), 3.54 (q, 2H, $^3J_{HH}$ = 7.2 Hz, CH_2CTp), 1.38 ppm (t, 3H, $^3J_{HH}$ = 7.2 Hz, CH_3CH$_2$C(pz)$_3$). ^{13}C{^{1}H} NMR (100.6 MHz, CDCl$_3$, 26 °C): δ = 153.1 (3-C(pz)), 133.1 (i-C(Ph)), 131.6 (5-C(pz)), 128.8 (*m*-C(Ph)), 128.3 (*p*-C(Ph)), 126.1 (*o*-C(Ph)), 103.7 (4-C(pz)), 93.1 (CTp), 34.1 (CH$_2$CTp), 9.3 ppm (CH$_3$CH$_2$). DRIFTS: $\tilde{\nu}_{max}$ = 3145vw, 3064vw, 3004vw, 2982vw, 2951vw, 2953w, 1604vw, 1582vw, 1528m, 1497m, 1457s, 1390s, 1358m, 1298m, 1275w, 1247w, 1217vs, 1180vw, 1160vw, 1100w, 1075m, 1051m, 1028m, 859s, 758s, 750s, 520vw cm^{-1}. Elemental analysis calcd (%) for C$_{30}$H$_{26}$N$_6$ (470.22 g mol^{-1}): C 76.57, H 5.57, N 17.86; found C 76.30, H 5.97, N 17.62.

nPrCTp^{3-Ph} (3f). Following the procedure described for **3a**, the crude product of **2e** (2.00 g, 4.52 mmol), Li[N(SiMe$_3$)$_2$] (983 mg, 5.88 mmol) and *n*PrI (553 μL, 5.88 mmol) yielded **3f** as a pale yellow solid as the crude product. Further purification was achieved by recrystallization from a 1 : 1 mixture of *n*-hexane and MTBE to afford **3f** as colourless crystals (2.13 g, 4.40 mmol, 97%) suitable for SCXRD analysis. ^{1}H NMR (400.1 MHz, CDCl$_3$, 26 °C): δ = 7.87 (m, 6H, *o*-H(Ph)), 7.39 (m, 9H, *m*-H(Ph), *p*-H(Ph)), 7.06 (d, 3H, $^3J_{HH}$ = 2.7 Hz, 5-H(pz)), 6.62 (d, 3H, $^3J_{HH}$ = 2.7 Hz, 4-H(pz)), 3.46 (m, 2H, CH_2CTp), 1.89 (m, 2H, CH_2CH$_2$CTp), 1.08 (t, 3H, $^3J_{HH}$ = 7.4 Hz, CH_3CH$_2$) ppm. ^{13}C{^{1}H} NMR (100.6 MHz, CDCl$_3$, 26 °C): δ = 153.1 (3-C(pz)), 133.1 (i-C(Ph)), 131.5 (5-C(pz)), 128.8 (*m*-C(Ph)), 128.3 (*p*-C(Ph)), 126.1 (*o*-C(Ph)), 103.7 (4-C(pz)), 92.8 (C(pz)$_3$), 42.5 (CH$_2$CTp), 17.8 (CH$_2$CH$_2$CTp), 14.4 (CH$_3$CH$_2$) ppm. DRIFTS: $\tilde{\nu}_{max}$ = 3059vw, 2961w, 2869vw, 1604vw, 1528m, 1499vs, 1455vs,

1435s, 1385s, 1357s, 1301s, 1279w, 1210vs, 1100w, 1074w, 1044w, 1028w, 946vw, 903m, 855m, 800w, 752s, 695s, 686m, 659vw, 627w, 511vw cm^{-1}. Elemental analysis calcd (%) for $C_{31}H_{28}N_6$ (484.2 g mol^{-1}): C 76.83, H 5.82, N 17.34; found C 76.35, H 5.69, N 17.43.

iBuCTp$^{3\text{-Ph}}$ (3g). Following the procedure described for **3a**, the crude product of **2e** (2.00 g, 4.52 mmol), Li[N(SiMe$_3$)$_2$] (983 mg, 5.88 mmol) and iBuI (676 μL, 5.88 mmol) yielded a pale yellow solid as the crude product. Further purification was achieved by recrystallization from MTBE to afford **3g** as colourless crystals (1.99 g, 3.98 mmol, 88%) suitable for SCXRD analysis. ^{1}H NMR (400.1 MHz, CDCl$_3$, 26 °C): δ = 7.85 (m, 6H, o-H(Ph)), 7.38 (m, 9H, m-H(Ph), p-H(Ph)), 7.02 (d, 3H, $^3J_{HH}$ = 2.7 Hz, 5-H(pz)), 6.61 (d, 3H, $^3J_{HH}$ = 2.7 Hz, 4-H(pz)), 3.45 (d, 2H, $^3J_{HH}$ = 5.4 Hz, CH$_2$CTp), 2.55 (m, 1H, (CH$_3$)$_2$CHCH$_2$CTp), 1.00 (d, 6H, $^3J_{HH}$ = 6.7 Hz, (CH$_3$)$_2$CH$_2$) ppm. ^{13}C{^{1}H} NMR (100.6 MHz, CDCl$_3$, 26 °C): δ = 152.8 (3-C(pz)), 133.1 (i-C(Ph)), 131.6 (5-C(pz)), 128.8 (m-C(Ph)), 128.3 (p-C(Ph)), 126.1 (o-C(Ph)), 103.9 (4-C(pz)), 93.3 (CTp), 47.6 (CH$_2$CTp), 24.5 ((CH$_3$)$_2$CHCH$_2$CTp), 24.1 ((CH$_3$)$_2$CH) ppm. DRIFTS: $\tilde{\nu}_{max}$ = 3145vw 3060vw, 2992vw, 2955w, 2867w, 1954vw, 1713vw, 1605vw, 1528m, 1499vs, 1456vs, 1387s, 1356s, 1288m, 1219s, 1208vs, 1102m, 1075m, 1045w, 1028vw, 975vw, 946w, 924w, 915w, 885w, 822w, 777w, 756s, 697s, 686w, 661vw, 627vw, 513 cm^{-1}. Elemental analysis calcd (%) for $C_{32}H_{30}N_6$ (498.3 g mol^{-1}): C 77.08, H 6.06, N 16.85; found C 76.53, H 5.92, N 16.49.

[(AlMe$_3$CTp$^{3\text{-}p\text{-}tBuPh}$)$_2$Mg] (4). A solution of Mg(AlMe$_4$)$_2$ (16.3 mg, 81.9 μmol) in 5 mL of n-hexane was added dropwise to a stirred suspension of the crude product of **2d** (100 mg, 164 μmol) in 5 mL of toluene. After stirring for 2 h the solvent was removed under reduced pressure yielding a white solid. Recrystallization from toluene gave **4** (47.8 mg, 34.5 μmol, 42%) as colourless crystals suitable for SCXRD analysis. ^{1}H NMR (400.1 MHz, [D$_8$]toluene, 26 °C): δ = 8.92 (d, 6H, $^3J_{HH}$ = 2.8 Hz, 5-H(pz)), 6.88 (m, 12H, o-H(Ph)), 6.69 (m, 12H, m-H(Ph)), 5.78 (d, 6H, $^3J_{HH}$ = 2.8 Hz, 4-H(pz)), 1.14 (s, 54H, C(CH$_3$)$_3$), 0.20 ppm (s, 18H, Al(CH$_3$)$_3$). ^{13}C{^{1}H} NMR (100.6 MHz, [D$_8$]toluene, 26 °C): δ = 156.3 (3-C(pz)), 151.5 (p-C(Ph)), 138.5 (3-C(pz)), 129.2 (i-C(Ph)), 128.3 (m-C(Ph)), 124.0 (o-C(Ph)), 105.0 (4-C(pz)), 87.6 (CAlMe$_3$), 34.4 (C(CH$_3$)$_3$), 31.2 (C(CH$_3$)$_3$), −2.2 ppm (Al(CH$_3$)$_3$). DRIFTS: $\tilde{\nu}_{max}$ = 3163w, 2964s, 2922m, 2868w, 1912vw, 1614vw, 1568vw. 1505m, 1474m, 1420w, 1378m, 1363w, 1344w, 1309vw, 1270w, 1248w, 1186s, 1020vw, 1005vw, 991vw, 949vw, 839m, 812s, 775vs, 744m, 731m, 695vs, 644w, 618vw, 561w, 523vw, 501w, 463vw, 429vw cm^{-1}. Elemental analysis calcd (%) for $C_{86}H_{108}Al_2MgN_{12} \cdot 0.5 C_7H_8$ (1434.37 g mol^{-1}): C 74.95 H 7.87 N 11.72; found: C 75.61 H 8.28 N 10.90. The carbon result is outside the range for analytical purity, but no better elemental analysis could be obtained to date, due to solvent molecules in the lattice and due to the highly air- and moisture-sensitive nature of compound **4**.

[(MeCTp$^{3\text{-Et}}$)$_2$Mg][AlMe$_4$]$_2$ (5a). A solution of Mg(AlMe$_4$)$_2$ (31.7 mg, 0.16 mmol) in 5 mL of n-hexane was added dropwise to a stirred suspension of **3a** (100 mg, 0.32 mmol) in 5 mL of toluene and a white precipitate formed immediately. After stir-

ring for 2 h the solvent was removed under reduced pressure and the residual solid was washed three times with n-pentane. **5a** was obtained as a white powder (121 mg, 0.14 mmol, 92%). Colourless crystals of **5a** suitable for SCXRD analysis were grown from THF at −40 °C. ^{1}H NMR (400.1 MHz, [D$_8$]THF, 26 °C): δ = 8.58 (d, 6H, ^3J(H,H) = 2.8 Hz; 5-H(pz)), 6.60 (d, 6H, $^3J_{HH}$ = 2.9 Hz; 4-H(pz)), 3.55 (s, 6H; CH$_3$CTp), 1.86 (q, 12H, $^3J_{HH}$ = 7.6 Hz; CH$_2$CH$_3$), 1.01 (t, 18H, $^3J_{HH}$ = 7.6 Hz; CH$_2$CH$_3$), −1.28 ppm (m, 24H; [Al(CH$_3$)$_4$]). ^{13}C{^{1}H} NMR (100.6 MHz, [D$_8$]THF, 26 °C): δ = 161.1 (3-C(pz)), 134.8 (5-C(pz)), 106.7 (4-C(pz)), 85.1 (MeCTp), 24.8 (CH$_3$CTp), 20.94 (CH$_2$CH$_3$), 12.15 (CH$_2$CH$_3$), −4.2 ppm (sext, ^1J(Al,C) = 70.4 Hz; [Al(CH$_3$)$_4$]). DRIFTS: $\tilde{\nu}_{max}$ = 3160vw, 2975vw, 2898m, 2798vw, 1528m, 1478w, 1436vw, 1411vw, 1386s, 1357w, 1314vw, 1298vw, 1212s, 1150w, 1080m, 1058w, 1025w, 994vw, 951vw, 796vw, 775m, 696s, 687m, 596vw, 546w, 488vw cm^{-1}. Elemental analysis calcd (%) for $C_{42}H_{72}Al_2MgN_6$ (823.39 g mol^{-1}): C 61.27, H 8.81, N 20.41; found: C 60.84, H 8.76, N 20.10.

[(MeCTp$^{3\text{-cyPr}}$)$_2$Mg][AlMe$_4$]$_2$ (5b) and [MeCTp$^{3\text{-cyPr}}$MgMe (thf)$_2$][AlMe$_4$] (6). A solution of **3b** (100 mg, 287 μmol) in 2 mL of toluene was added dropwise to a solution of Mg(AlMe$_4$)$_2$ (57.0 mg, 287 μmol) in 5 mL of toluene and a white precipitate formed immediately. After removing the solvent under reduced pressure, the crude product was washed with n-pentane (3 × 3 mL) to yield [(MeCTp$^{3\text{-cyPr}}$)$_2$Mg][AlMe$_4$]$_2$ (5b) as a white powder. Colourless crystals suitable for SCXRD analysis could be obtained by heating the solid in a J. Young valve NMR tube to 150 °C in toluene. Elemental analysis calcd (%) for $C_{48}H_{72}Al_2MgN_{12} \cdot C_8H_{24}MgAl_2$ (1094.01 g mol^{-1}): C 61.48 H 8.85 N 15.36; found: C 61.16 H 8.52 N 15.11 (crude product). Because of the high insolubility of **5b** in aliphatic and aromatic solvents, no satisfactory NMR spectra could be obtained. Redissolving **5b** in THF and cooling to −40 °C led to the formation of colourless crystals of **6** suitable for SCXRD analysis. ^{1}H NMR (400.1 MHz, [D$_8$]THF, 26 °C): δ = 8.36 (d, 3H, $^3J_{HH}$ = 2.7 Hz, 5-H(pz)), 6.09 (d, 3H, $^3J_{HH}$ = 2.4 Hz, 4-H(pz)), 3.40 (s, 3H, CH$_3$C(pz)$_3$), 1.12 (m, 3H, (CH$_2$)$_2$CH), 0.67 (m, 12H, (CH$_2$)$_2$CH) ppm. ^{13}C{^{1}H} NMR (100.6 MHz, CDCl$_3$, 26 °C): δ = 163.2 (3-C(pz)), 133.9 (5-C(pz)), 101.3 (4-C(pz)), 84.1 (C(pz)$_3$), 23.8 (CH$_3$C(pz)$_3$), 10.9 ((CH$_2$)$_2$CH), 9.40 ((CH$_2$)$_2$CH), −4.8 (sext, $^1J_{C,Al}$ = 70.4 Hz, Al(CH$_3$)$_4$) ppm.

[(MeCTp$^{3\text{-Cy}}$)Mg(AlMe$_4$)][AlMe$_4$] (8). A solution of Mg (AlMe$_4$)$_2$ (42.0 mg, 0.21 mmol) in 5 mL of n-hexane was added dropwise to a stirred suspension of **3c** (100 mg, 0.21 mmol) in 5 mL of toluene. After stirring for 2 h, the solvent was removed under reduced pressure yielding a white solid. Redissolving the solid in anhydrous 1,2-difluorobenzene and cooling to −40 °C afforded colourless crystals of **8** (66.5 mg, 0.10 mmol, 46%) suitable for SCXRD analysis. ^{1}H NMR (400.1 MHz, [D$_8$] toluene, 26 °C): δ = 7.84 (m, 3H; 5-H(pz)), 5.80 (m, 3H; 4-H(pz)), 3.11 (s, 3H; CH$_3$CTp), 2.69 (m, 3H; 1-CH(Cy)), 1.59 (m, 12H; 2,6-; 3,5-CH$_2$(Cy)), 1.52 (m, 3H; 4-CH$_2$(Cy)), 1.21 (m, 6H; 3,5-CH$_2$(Cy)), 1.06 (m, 9H; 2,6-; 3,5-CH$_2$(Cy)), −0.19 ppm (s, 24H; [Al(CH$_3$)$_4$]/Mg(CH$_3$)$_2$Al(CH$_3$)). ^{13}C{^{1}H} NMR (100.6 MHz, [D$_8$]toluene/1,2-difluorobenzene, 26 °C): δ = 164.4 (3-C(pz)), 133.1 (5-C(pz)), 105.1 (4-C(pz)), 83.5 (MeCTp), 37.5 (1-C(Cy)),

33.4 (2,6-C(Cy)), 26.3 (3,5-C(Cy)), 25.7 (4-C(Cy)), 24.9 (CH_3CTp), −4.2 ppm ([Al(CH_3)$_4$]/Mg(CH_3)$_3$Al(CH_3)). DRIFTS: $\tilde{v}_{max}$ = 3147w, 2922vs, 2850m, 2797w, 1530s, 1507vw, 1479w, 1447m, 1414w, 1397w, 1378m, 1360m, 1346w, 1303vw, 1290vw, 1268vw, 1211vs, 1185w, 1142m, 1078vs, 1031m, 996vw, 967vw, 890vw, 851vw, 812vw, 791w, 767vs, 743w, 723s, 705vs, 694vs, 613s, 548w, 419w cm^{-1}. Elemental analysis calcd (%) for $C_{37}H_{66}Al_2MgN_6$ (689.29 g mol^{-1}): C 66.01, H 9.88, N 12.48; found: C 65.96 H 10.10 N 12.37.

[(MeCTp$^{3\text{-}p\text{-}t\text{BuPh}}$)Mg(AlMe$_4$)][AlMe$_4$] (9). A solution of Mg (AlMe$_4$)$_2$ (42.8 mg, 0.22 mmol) in 5 mL of n-hexane was added dropwise to a stirred suspension of **3d** (135 mg, 0.22 mmol) in 5 mL of toluene. After stirring for 2 h the solvent was removed under reduced pressure yielding a yellow oil. Redissolving the oil in anhydrous benzene and adding n-pentane dropwise under stirring at 40 °C afforded colourless crystals of **9** (134 mg, 0.16 mmol, 79%) suitable for SCXRD analysis. ^{1}H NMR (400.1 MHz, [D$_8$]toluene, 26 °C): δ = 8.03 (m, 3H; 5-H(pz)), 7.31 (m, 6H; o-H(Ph)), 7.23 (m, 6H; m-H(Ph)), 6.28 (m, 3H; 4-H(pz)), 3.27 (s, 3H; CH_3CTp), 1.12 (s, 27H; C(CH_3)$_3$), −0.34 ppm (s, 24H; [Al(CH_3)$_4$]/Mg(CH_3)$_2$Al(CH_3)). ^{13}C{^{1}H} NMR (100.6 MHz, [D$_8$]toluene/1,2-difluorobenzene, 26 °C): δ = 158.7 (3-C(pz)), 154.4 (p-C(Ph)), 133.4 (5-C(pz)), 129.2 (ipso-C(Ph)), 128.3 (o-C(Ph)), 126.5 (m-C(Ph)), 107.5 (4-C(pz)), 84.6 (MeCTp), 34.8 (C(CH$_3$)$_3$), 31.0 (C(CH_3)$_3$), 25.2 (CH_3CTp), −4.5 ppm ([Al(CH_3)$_4$]/Mg(CH_3)$_2$Al(CH_3)$_2$). DRIFTS: $\tilde{v}_{max}$ = 3147w, 2962m, 2906m, 2870w, 2800w, 1615w, 1541m, 1505m, 1468w, 1383m, 1364w, 1304vw, 1260w, 1212m, 1153vw, 1127vw, 1098vw, 1066m, 1017vw, 991vw, 947vw, 839vw, 775s, 698m, 688s, 623w, 541vw, 501vw cm^{-1}. Elemental analysis calcd (%) for $C_{49}H_{72}Al_2MgN_6$ (823.43 g mol^{-1}): C 71.47, H 8.81, N 10.21; found: C 71.97, H 8.13, N 10.94. The hydrogen result is outside the range for analytical purity, but no better elemental analysis could be obtained to date due to solvent molecules in the lattice and the highly air- and moisture-sensitive nature of compound **9**.

[MeC(pz$^{3\text{-}p\text{-}t\text{BuPh}}$)$_2$(pz$^{3\text{-}p\text{-}t\text{BuPh,5-AlMe}_3}$)]MgMe (10). A solution of **9** (144.2 mg, 0.18 mmol) in benzene was heated in a pressure tube to 90 °C for 1 d. The mixture was allowed to cool to ambient temperature and the solvent was removed under reduced pressure. Redissolving the obtained solid in toluene and slow evaporation of the solvent led to colourless crystals of **10** (84.9 mg, 0.12 mmol, 66%) suitable for SCXRD analysis. ^{1}H NMR (400.1 MHz, [D$_8$]benzene, 26 °C): δ = 7.45 (m, 2H, o-H(Ph, pz$^{3\text{-}p\text{-}t\text{BuPh,5-AlMe}_3}$)), 7.41 (m, 4H, o-H(Ph, pz$^{3\text{-}p\text{-}t\text{BuPh}}$)), 7.32 (s, 1H, 4-$H$(pz, pz$^{3\text{-}p\text{-}t\text{BuPh,5-AlMe}_3}$)), 7.18 (m, 6H, 5-$H$(pz, pz$^{3\text{-}p\text{-}t\text{BuPh}}$) and m-H(Ph, pz$^{3\text{-}p\text{-}t\text{BuPh}}$)), 7.06 (m, 2H, m-H(Ph, pz$^{3\text{-}p\text{-}t\text{BuPh,5-AlMe}_3}$)), 5.90 (d, 2H, 4-$H$(pz, pz$^{3\text{-}p\text{-}t\text{BuPh}}$)), 3.35 (s, 3H, C$H_3$), 1.08 (s, 18H, C(C$H_3$)$_3$(pz$^{3\text{-}p\text{-}t\text{BuPh}}$)), 1.06 (s, 9H, C(C$H_3$)$_3$(pz$^{3\text{-}p\text{-}t\text{BuPh,5-AlMe}_3}$)), 0.16 (s, 9H, Al(C$H_3$)$_3$), −0.99 ppm (s, 3H, MgC$H_3$). ^{13}C{^{1}H} NMR (100.6 MHz, [D$_8$]toluene/1,2-difluorobenzene, 26 °C): δ = 156.7 (3-C(pz, pz$^{3\text{-}p\text{-}t\text{BuPh}}$)), 156.5 (3-$C$(pz, pz$^{3\text{-}p\text{-}t\text{BuPh,5-AlMe}_3}$)), 153.7 ($p$-$C$(Ph, pz$^{3\text{-}p\text{-}t\text{BuPh}}$)), 152.2 ($p$-$C$(Ph, pz$^{3\text{-}p\text{-}t\text{BuPh,5-AlMe}_3}$)), 132.1 (5-$C$(pz, pz$^{3\text{-}p\text{-}t\text{BuPh}}$)), 128.2 (4-$C$(pz, pz$^{3\text{-}p\text{-}t\text{BuPh,5-AlMe}_3}$)), 128.0 ($o$-$C$(Ph, pz$^{3\text{-}p\text{-}t\text{BuPh}}$)), 126.3 ($m$-$C$(Ph, pz$^{3\text{-}p\text{-}t\text{BuPh}}$)), 126.0 ($m$-$C$(Ph, pz$^{3\text{-}p\text{-}t\text{BuPh,5-AlMe}_3}$)), 105.7 (4-

C(pz, pz$^{3\text{-}p\text{-}t\text{BuPh}}$)), 87.4 (Me$C$Tp), 34.7 ($C$(CH$_3$)$_3$ (pz$^{5\text{-H}}$)), 34.6 (C(CH$_3$)$_3$(pz$^{3\text{-}p\text{-}t\text{BuPh,5-AlMe}_3}$)), 31.1 ($C$(CH$_3$)$_3$(pz$^{3\text{-}p\text{-}t\text{BuPh}}$)), 31.1 ($C$(CH$_3$)$_3$(pz$^{3\text{-}p\text{-}t\text{BuPh,5-AlMe}_3}$)), 26.7 ($CH_3$CTp), −4.6 ppm (AlMe$_3$). The ^{13}C NMR resonances for Mg-CH_3, both quaternary ipso-Ph carbons, the o-Ph carbon of the pz$^{3\text{-}p\text{-}t\text{BuPh,5-AlMe}_3}$ and the 5-C(pz$^{5\text{-AlMe}_3}$) could not be detected due to overlap with the solvent signal or insufficient resolution. Elemental analysis calcd (%) for $C_{45}H_{59}AlMgN_6$ (735.3 g mol^{-1}): C 73.54, H 8.45, N 11.19; found: C 74.88, H 8.44, N 10.11.

[(MeCTp$^{3\text{-}p\text{-}t\text{BuPh}}$)MgMe][AlMe$_4$] (11). Solid **9** converted to complex **11**, either over 6 months at ambient temperature or after 4 d under reduced pressure. Compound **11** was obtained quantitatively as a white solid. ^{1}H NMR (400.1 MHz, [D$_8$] toluene, 26 °C): δ = 8.28 (m, 3H; 5-H(pz)), 7.34 (m, 6H; o-H(Ph)), 7.16 (m, 6H; m-H(Ph)), 6.33 (m, 3H; 4-H(pz)), 3.54 (s, 3H; CH_3CTp), 1.08 (s, 27H; C(CH_3)$_3$), −0.09 (s, 12H; Al(CH_3)$_4$), −1.04 ppm (s, 3H, MgCH_3). ^{13}C{^{1}H} NMR (100.6 MHz, [D$_8$] toluene/1,2-difluorobenzene, 26 °C): δ = 158.2 (3-C(pz)), 153.9 (p-C(Ph)), 134.3 (5-C(pz)), 129.2 (ipso-C(Ph)), 128.3 (o-C(Ph)), 126.2 (m-C(Ph)), 107.1 (4-C(pz)), 85.0 (MeCTp), 34.7 (C(CH$_3$)$_3$), 31.0 (C(CH_3)$_3$), 25.6 ppm (CH_3CTp). The carbon signal of the methyl group coordinated to the magnesium centre could not be detected. Elemental analysis calcd (%) for $C_{45}H_{59}AlMgN_6$ (735.3 g mol^{-1}): C 73.51, H 8.09, N 11.43; found: C 73.40, H 8.14, N 10.62. The nitrogen result is outside the range for analytical purity, but no better elemental analysis could be obtained to date due the highly air- and moisture-sensitive nature of compound **11**.

Data availability

The data supporting this article have been included as part of the ESI.† Crystallographic data for the compounds have been deposited in the Cambridge Crystallographic Data Centre (2386219–2386230).†

Conflicts of interest

There are no conflicts of interest.

Acknowledgements

References

1 V. Grignard, *C. R. Hebd. Seances Acad. Sci.*, 1900, **130**, 1322–1325.
2 E. C. Ashby, *Q. Rev., Chem. Soc.*, 1967, **21**, 259.
3 F. Bickelhaupt, *Angew. Chem., Int. Ed. Engl.*, 1974, **13**, 419–420.

4 E. C. Ashby, J. Laemmle and H. M. Neumann, *Acc. Chem. Res.*, 1974, **7**, 272–280.

5 F. Bickelhaupt, *Angew. Chem.*, 1987, **99**, 1020–1035.

6 M. Orchin, *J. Chem. Educ.*, 1989, **66**, 586.

7 P. R. Markies, R. M. Altink, A. Villena, O. S. Akkerman, F. Bickelhaupt, W. J. J. Smeets and A. L. Spek, *Adv. Organomet. Chem.*, 1991, **402**, 289–312.

8 G. S. Silverman and P. E. Rakita, *Handbook of Grignard Reagents*, CRC Press, 1996.

9 W. Schlenk and W. Schlenk Jr., *Chem. Ber.*, 1929, **62**, 920–924.

10 A. C. Cope, *J. Am. Chem. Soc.*, 1935, **57**, 2238–2240.

11 E. Weiss, *J. Organomet. Chem.*, 1964, **2**, 314–321.

12 J. Toney and G. D. Stucky, *J. Organomet. Chem.*, 1970, **22**, 241–249.

13 T. Greiser, J. Kopf, D. Thoennes and E. Weiss, *J. Organomet. Chem.*, 1980, **191**, 1–6.

14 H. Viebrock and E. Weiss, *J. Organomet. Chem.*, 1994, **191**, 121–126.

15 R. I. Yousef, B. Walfort, T. Rüffer, C. Wagner, H. Schmidt, R. Herzog and D. Steinborn, *J. Organomet. Chem.*, 2005, **690**, 1178–1191.

16 O. Michel, C. Meermann, K. W. Törnroos and R. Anwander, *Organometallics*, 2009, **28**, 4783–4790.

17 A. K. Bartholomew, L. M. Guard, N. Hazari and E. D. Luzik, *Aust. J. Chem.*, 2013, **66**, 1455–1458.

18 W. Hückel and H. Bretschneider, *Ber. Dtsch. Chem. Ges.*, 1937, **70**, 2024–2026.

19 S. Trofimenko, *J. Am. Chem. Soc.*, 1966, **88**, 1842–1844.

20 S. Trofimenko, *J. Am. Chem. Soc.*, 1967, **89**, 3170–3177.

21 S. Trofimenko, *J. Am. Chem. Soc.*, 1967, **89**, 6288–6294.

22 S. Trofimenko, J. C. Calabrese, J. K. Kochi, S. Wolowiec, F. B. Hulsbergen and J. Reedijk, *Inorg. Chem.*, 1992, **31**, 3943–3950.

23 S. Trofimenko, *Chem. Rev.*, 1993, **93**, 943–980.

24 A. L. Rheingold, R. L. Ostrander, B. S. Haggerty and S. Trofimenko, *Inorg. Chem.*, 1994, **33**, 3666–3676.

25 C. López, D. Sanz, R. M. Claramunt, S. Trofimenko and J. Elguero, *J. Organomet. Chem.*, 1995, **503**, 265–276.

26 S. Trofimenko, A. L. Rheingold and L. M. Liable Sands, *Inorg. Chem.*, 2002, **41**, 1889–1896.

27 S. Trofimenko, *in Progress in Inorganic Chemistry*, John Wiley & Sons, Ltd, 2007, pp. 115–210.

28 S. Krieck, A. Koch, K. Hinze, C. Müller, J. Lange, H. Görls and M. Westerhausen, *Eur. J. Inorg. Chem.*, 2016, **2016**, 2332–2348.

29 H. R. Bigmore, J. Meyer, I. Krummenacher, H. Rüegger, E. Clot, P. Mountford and F. Breher, *Chem. – Eur. J.*, 2008, **14**, 5918–5934.

30 M. G. Cushion, J. Meyer, A. Heath, A. D. Schwarz, I. Fernández, F. Breher and P. Mountford, *Organometallics*, 2010, **29**, 1174–1190.

31 J. Meyer, I. Kuzu, S. González-Gallardo and F. Breher, *Z. Anorg. Allg. Chem.*, 2013, **639**, 301–307.

32 J. Meyer, S. González-Gallardo, S. Hohnstein, D. Garnier, M. K. Armbruster, K. Fink, W. Klopper and F. Breher, *Chem. – Eur. J.*, 2015, **21**, 2905–2914.

33 C. Müller, A. Koch, H. Görls, S. Krieck and M. Westerhausen, *Inorg. Chem.*, 2015, **54**, 635–645.

34 R. Lalrempuia, A. Stasch and C. Jones, *Chem. – Asian J.*, 2015, **10**, 447–454.

35 C. Stuhl, C. Maichle-Mössmer and R. Anwander, *Chem. – Eur. J.*, 2018, **24**, 14254–14268.

36 M. Veith, *Eur. J. Inorg. Chem.*, 2000, **2000**, 1883–1899.

37 S. Harder, F. Feil and T. Repo, *Chem. – Eur. J.*, 2002, **8**, 1991–1999.

38 S. Juliá, J. M. del Mazo, L. Avila and J. Elguero, *Org. Prep. Proced. Int.*, 1984, **16**, 299–307.

39 D. L. Reger, T. C. Grattan, K. J. Brown, C. A. Little, J. J. S. Lamba, A. L. Rheingold and R. D. Sommer, *J. Organomet. Chem.*, 2000, **607**, 120–128.

40 P. Ghosh and G. Parkin, *Inorg. Chem.*, 1996, **35**, 1429–1430.

41 K. Ziegler and E. Holzkamp, *Liebigs Ann. Chem.*, 1957, **605**, 93–97.

42 J. L. Atwood and G. D. Stucky, *J. Am. Chem. Soc.*, 1969, **91**, 2538–2543.

43 B. Wrackmeyer and E. V. Klimkina, *Z. Naturforsch., B: J. Chem. Sci.*, 2014, **63**, 923–928.

44 O. Michel, H. M. Dietrich, R. Litlabø, K. W. Törnroos, C. Maichle-Mössmer and R. Anwander, *Organometallics*, 2012, **31**, 3119–3127.

45 C. Stuhl and R. Anwander, *Dalton Trans.*, 2018, **47**, 12546–12552.

46 A. D. Pajerski, M. Parvez and H. G. Richey, *J. Am. Chem. Soc.*, 1988, **110**, 2660–2662.

47 M. Vestergren, J. Eriksson and M. Håkansson, *Chem. – Eur. J.*, 2003, **9**, 4678–4686.

48 A. Jaenschke, J. Paap and U. Behrens, *Z. Anorg. Allg. Chem.*, 2008, **634**, 461–469.

49 J. A. Bilbrey, A. H. Kazez, J. Locklin and W. D. Allen, *J. Comput. Chem.*, 2013, **34**, 1189–1197.

50 R. Lalrempuia, A. Stasch and C. Jones, *Chem. – Asian J.*, 2015, **10**, 447–454.

51 U. Wannagat and H. Niederprüm, *Angew. Chem.*, 1959, **71**, 574–574.

52 B. M. Ahmed and G. Mezei, *RSC Adv.*, 2015, **5**, 24081–24093.

53 A.-K. Pleier, H. Glas, M. Grosche, P. Sirsch and W. R. Thiel, *Synthesis*, 2001, 55–62.